

Measuring dose profiles and surface dose rates of sealed pure-beta sources to determine radioactivity

Seongmoon Jung^{a,b}, Chang Heon Choi^d and Sung-Joon Ye^{a,c,d*}

^aProgram in Biomedical Radiation Sciences, Department of Transdisciplinary Studies,
Graduate School of Convergence Science and Technology, Seoul National University, Seoul, Korea

^bBiomedical Research Institute, Seoul National University Hospital, Seoul, Korea

^cInterdisciplinary Program in Radiation Applied Life Science,
Seoul National University College of Medicine, Seoul, Korea

^dDepartment of Radiation Oncology, Seoul National University Hospital, Seoul, Korea

*Corresponding author: sye@snu.ac.kr

1. Introduction

Radioisotopes have been widely used in forms of isotopic tracers, labeled compounds and sealed sources [1,2]. In general, radioisotopes are produced by a nuclear reactor and a charged-particle accelerator. A beta-emitter of radioisotope has been used for therapeutics and diagnostics in medicine. This radionuclide has been also used as fertilizer tracking, thickness gauges and nuclear battery in industrial application. In other words, the demand for associated radioisotope industry has been rising. One of the most important specifications of radioisotope is a radioactivity. Therefore, determining the methodology of radioactivity assay is also becoming an important procedure [3].

The advancement of the sciences associated with radiation detection has contributed to the development of more sensitive, reliable and user-friendly calibration systems. The gas-flow proportional counters, liquid scintillation counters, HP-Ge detectors and ionization chambers have been considered to be necessary for the primary calibration systems of radioactivity [4,5].

The proportional counter is a type of gas-filled detector and designed to measure a detector output that is proportional to the incident radiation energy. This detector has high accuracy and efficiency in measuring an emitting rate of betas. Using a gas-flow proportional counter, the source size should not be larger than a sensitive area determined by the detector geometry. Further the calibration measurement is limited to the source with a radioactivity of less than 20 kBq [6]. But the radioactivity of a beta-source in general use is often up to a few MBq.

On the other hand, a liquid scintillation detector can be used only to measure a radioactivity of liquid mixture isotopes [7,8]. Therefore, it can't be used to measure the radioactivity of a sealed beta-source intact. In general it is difficult to measure a radioactivity of beta-isotope accurately due to self-absorption and scattering. A destructive dissolution of a sealed beta-source into liquid scintillation techniques to determine an actually-contained radioactivity can only give a reasonably accurate radioactivity.

Consequently, using the current methods the measurement of actually-contained radioactivity within an encapsulated beta-source is prone to damage and has limitations on its physical size and strength of radioactivity.

In previous study we developed a convenient and novel method to accurately determine a radioactivity of a standard sealed pure beta-source [10]. It was based on an assumption that the surface dose rate of an encapsulated pure beta-source is proportional to the radioactivity of it. Hence, the radioactivity of the pure beta-source can be determined by measuring the surface dose rate and the correction factor associated with the geometry and materials of the source and the detector. Finally, we applied this method to determine an unknown radioactivity of a Sr/Y-90 test source manufactured by the HANARO reactor group of KAERI (Korea Atomic Energy Research Institute).

2. Methods and Results

2.1 Hypothesis

An electron flux emitted by a sealed pure-beta source is proportional to a radioactivity of the source and the surface dose rate of the source is proportional to the electron flux when the collision stopping power is constant as follows (Equation 1):

$$\dot{D} = \Phi \cdot \left(\frac{S_{col}}{\rho} \right) \quad (1)$$

Thus, the radioactivity of the source is proportional to the surface dose rate of it as well. If a conversion factor defined by the ratio of surface dose rate to radioactivity is given, then the radioactivity of a source can be determined by dividing a measured surface dose rate by the conversion factor [Fig. 1].

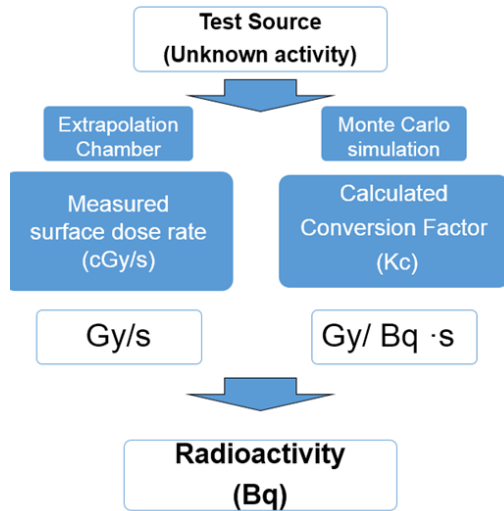


Fig. 1 Schematic diagram to determine a radioactivity of sealed test beta source

2.2 Test Source

A sealed test source of Sr/Y-90 source was designed by Korea Atomic Energy Research Institute (KAERI) and generated in the HANARO reactor of KAERI. Fig.2 shows a schematic diagram of the test source and pictures of test source. The source activity was housed in an absorbent (ZrO_2) of 0.3 mm in thickness and 11 mm in diameter. The liquid containing Sr/Y-90 was dropped into the absorbent disk and then evaporated the liquid leaving Sr/Y-90. These sources were also prepared from a weighted aliquot of solution whose radioactivity in ci/g was determined using a liquid scintillation counter. A stainless steel (STS 304) window film (0.1mm thickness) below the absorbent disk was located to encapsulate the activity. The components were encapsulated by stainless steel (STS 304) and the capsule was 5 mm in height and 15mm in diameter. The contained radioactivity of the test source was 5.826 kBq on 06-Oct-14.

We should check the source distribution of test source. It is very hard to distribute source uniformly on absorbent disk. The source distribution should be described in Monte Carlo simulations according realistic source distribution. The active surface of the test source was attached with radiochromic film to measure the uniformity of radioactivity distribution. The dose profile was obtained with direction center to peripheral and interval of 45 degrees. These 8 profiles were averaged. The profile of test source was determined by this half averaged profile. The measured radioactivity distribution was also reflected in obtaining a conversion factor from Monte Carlo simulations.

In MCNP5, SCn card is available for source probability distribution. A mnemonic SPn is used to specify the source probability. A function number and input parameter of SPn card have connection with distribution of source probability. In this simulation, the

function number was determined as 'twenty one' for describing radial distribution. The radial source distribution was described by power law. An input parameter of source probability in MCNP5 was adjusted to minimize the difference in the radioactivity distributions between measurement and simulation.

As mentioned in the previous study, Monte Carlo simulations and dose rate measurements were performed to determine radioactivity. The K_c of the test source was determined by assuming uniform and measured realistic dose distributions for comparison. Monte Carlo simulations were performed to predict an appropriate SDD for the test source. The test source was described according diagram provided by KAERI.

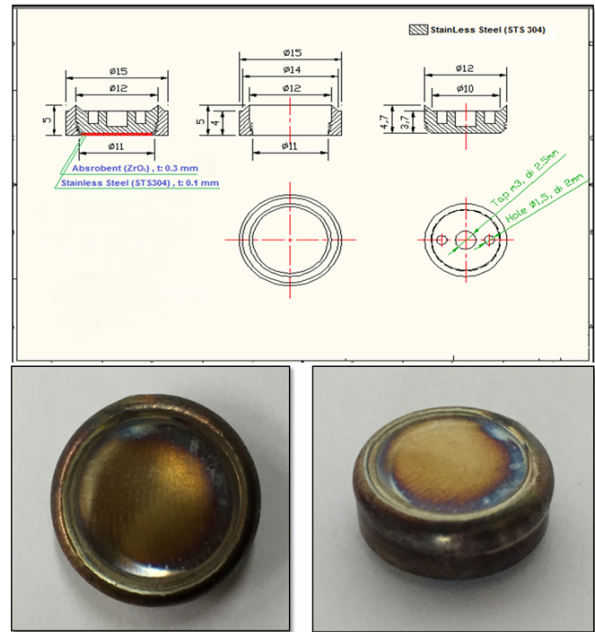


Fig.2 The schematic diagram (upper) and pictures of test source (lower)

2.3 Extrapolation Chamber

The surface dose rates of test source were determined using an extrapolation chamber (Bohm extrapolation chamber, PTW, Germany). An extrapolation chamber can vary its ionization volume to a vanishingly small amount. In the measurements, the spacing air gaps were in the range of 1.0, 1.5, 2.0, 3.0, 4.0, 5.0 mm. The absorbed dose rate in water, D_w , was determined from the slope of the linear fitting (i.e., extrapolation curve), the change of the ionization chamber current (I) vs chamber air gap thickness (t). All readings were normalized to a reference temperature (20°C) and pressure (101.325 kPa). The absorbed dose rate in water was given as below:

$$\dot{D}_w = \frac{\left(\frac{W}{e}\right) S_{w,air}}{\rho_0 a} \left(\frac{\Delta I}{\Delta t}\right)_{t \rightarrow 0} k_{back} \quad (2)$$

where (W/e) = the mean energy required to produce an ion pair in dry air divided by the elementary charge (33.83 ± 0.06 J/C), ρ_0 = the density of air (1.2047kg/m^3) in the reference condition, a = the area of the collecting electrode (7.0685 cm^2), $S_{w,air}$ = the ratio of the mean mass-collision stopping power of water to that of air, $(\Delta I/\Delta t)_{t \rightarrow 0}$ = the rate of change of current (I) with the distance (t , i.e., the extrapolation chamber electrode's air gap). The measurements were repeated at five different SDDs (source-to-detector distance) of 11, 13, 15 and 17 mm within 0.1 mm precision.

2.4 Monte Carlo Simulations

Monte Carlo simulations were carried out using the MCNP5 code that the physics and algorithms were well known and validated in our previous papers and others [10,11]. The MCNP code employed an improved electron transport algorithm of ITS 3.0 (Integrated Tiger Series Version 3.0) [12]. The beta spectra used in the coupled photon/electron transport were the data of Brookhaven National Laboratory Report [13]. Photons and electrons were tracked until they reached the cutoff energy of 1 keV. We assumed that the source radioactivity was uniformly distributed in the entire volume of absorbent disk. In order to reach statistical errors less than 2.5% for any voxels of interest in the simulation geometry, the number of histories was adjusted on a Linux cluster ($2.67\text{ GHz} \times 24\text{ CPUs}$).

We determined the minimum distance between the detector and source surfaces to make that the radiation field at the detector surface be larger than the area of collecting electrode. Therefore, we simulated the field size at the entrance window of extrapolation chamber for various SDDs. The cylindrical cell of a 30 mm diameter and 1 mm thickness was set at the entrance window using F8 tally. The dose distribution in the cell was calculated to confirm the field size requirement for EC.

For a disk source parallel to a circular detector, only some of emitting particles have a chance to enter the detector through a solid angle given by the size and shape of the source and detector, and the distance between them. Also some particles emitted from the source can be scattered and absorbed with the media (including air) between the source and the detector. Thus, the measured data have to be corrected to determine the total number of particles emitted from the source. Monte Carlo simulations of this situation would be a practical solution to determine these correction factors. The detector efficiency was defined as the ratio of particles emitted from the source to particles arrived at the detector. The detector efficiencies for various SDDs were determined by using the surface current tally (F1) of MCNP5. The surface of circular type with a 30 mm diameter was set at four different distances (11, 13, 15 and 17 mm) from the source in air. All

measurement results were corrected by these calculated detector efficiencies.

The energy spectrum of beta-particles emitted from the source was moderated, since beta-particles were interacted by the source material itself and the metallic encapsulation. The change in the energy spectrum was calculated with the surface flux tally (F2) of MCNP5 using the tally energy card (En). The energy range of zero to the maximum values of Sr/Y-90 betas was separated into 22 and 17 bins with the same interval (0.1 MeV). The energy spectrum was calculated at 0.5 mm depth in water from the surface of source. The energy spectrum in a cylindrical cell of a 30 mm diameter and 0.1 mm thickness was calculated to obtain the stopping power ratio of water to air, which was used to determine the dose rate at the reference depth. The shape and dimension of the cell were similar to the air cavity of an extrapolation chamber (EC) used in the surface dose measurements. To calculate the dose rates under the same condition with measurements, the standard sources was placed in air at SDD = 11, 13, 15 and 17 mm from an extrapolation chamber. In addition, the pulse height tally (*F8) of MCNP5 was used to determine the dose rate at the reference depth (0.5 mm) in water. The same shape and dimension of the cell that was used for the energy spectrum calculation was used to calculate the dose rate. The calculated dose rates were obtained for the four different SDDs (11, 13, 15 and 17 mm). The result obtained by *F8 tally was energy deposit per history that was equal to dose per radioactivity

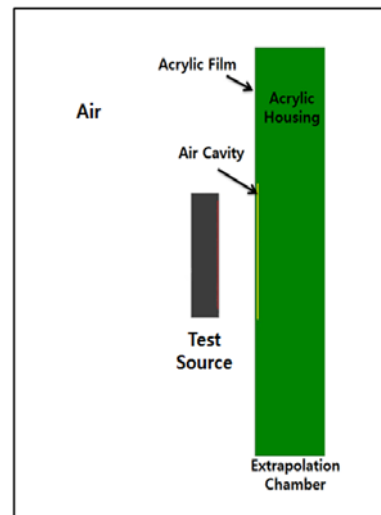


Fig.3 Monte Carlo simulation geometry

3. Results

Three test sources were produced by KAERI to validate developed method. Fig. 4 shows film measurement and dose distribution of these test sources. Fig. 4(a) and (b) show an irregular dose distribution. This distribution couldn't be described in Monte Carlo simulation. Fig. 4(c) shows a concave dose distribution.

This distribution could be described by adjusting input parameter of SPn card in Monte Carlo simulation. Therefore, the test source with concave dose distribution was selected to determine the radioactivity using developed method in this study.

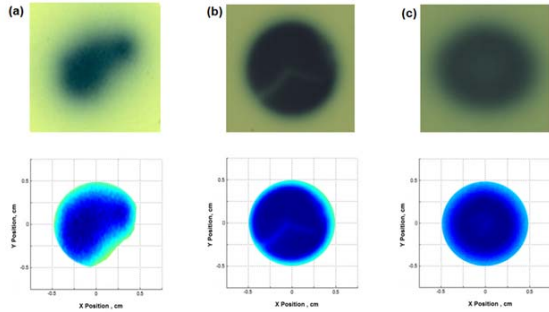


Fig. 4 Film measurements and dose distributions of three test sources produced by KAERI. (a) and (b) shows irregular dose distributions while (c) has a concave dose distribution.

Due to the radial symmetry of radioactivity distribution, the dose profile was obtained along the direction from the center of the disk to peripheries at an interval of 45 degree. These eight profiles were averaged for simple use of MC simulations in Fig. 5(b). Based on this realistic non-uniform profile of radioactivity, the input parameter of SPn card was determined as 1.14 to describe the distribution of source probability. The calculated conversion factor (K_c) was 1.69×10^{-08} cGy/s·Bq. Assuming an uniformity of radioactivity, the calculated conversion factor (K_c) was 8% higher than that based on the non-uniformity. Table 1 shows a difference in K_c between uniform and non-uniform distributions for four different SDDs.

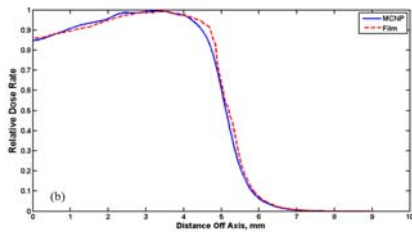


Fig. 5 Dose profiles from film and MCNP of the test source having a concave dose distribution (Fig 4(c))

SDD (mm)	Energy deposit per history (cGy / history)	
	Uniform	Non-uniform
11	1.79×10^{-08}	1.66×10^{-08}
13	1.81×10^{-08}	1.68×10^{-08}
15	1.83×10^{-08}	1.71×10^{-08}
17	1.84×10^{-08}	1.70×10^{-08}
Mean	1.81×10^{-08}	1.69×10^{-08}

Table 1 The calculated conversion factors (K_c) of test sources with uniform and realistic non-uniform dose distributions

Fig. 6 shows extrapolation curves of the test source for the four different SDDs. These distances were determined by MC. At these distances, we confirmed the radiation field was larger than the electrode size.

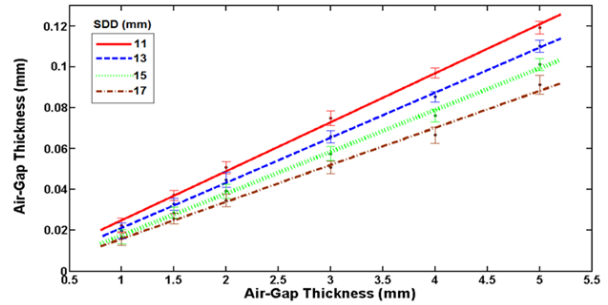


Fig. 6 Extrapolation chamber current vs air-gap thickness between two chamber electrodes at four source-to-detector distances for the selected Sr/Y-90 test source

Table 2 summarized the detector efficiencies and the dose rates corrected by efficiencies for the four different SDDs. The average dose rate of the test source was 7.04×10^{-05} cGy/s. Therefore, the radioactivity of the test source was determined to be 4.166 kBq. The radioactivity reported by the manufacturer was 5.803 kBq at the time of this study. There is 39% difference between determined radioactivity by proposed method and certificated radioactivity by manufacturer.

SDD (mm)	Slope of the extrapolation curve (pA/mm)	Detector Efficiency	Corrected Dose rate (cGy/s)
11	0.0269	0.179	7.10×10^{-05}
13	0.0225	0.151	7.04×10^{-05}
15	0.0188	0.127	6.95×10^{-05}
17	0.0161	0.107	7.06×10^{-05}
Mean			7.04×10^{-05}

Table 2 Slope of the extrapolation chamber curve obtained by EC measurement, the detection efficiencies and corrected dose rates for four source-to-detector distances

4. Conclusions

The method developed in this study was applied to determine a radioactivity of Sr/Y-90 test source. The radioactivity determined by this method was about 39% lower than one reported by the manufacturer. This difference might result from the lack of accuracy in determining the radioactivity of the original source liquid and the amount of liquid dropped on the absorbent disk. Furthermore, accuracy in the calculated conversion factor mainly relies on how closely to simulate a sealed source and a detector in MCNP. The geometry and compositions of the test source given by

the manufacturer were described in our MCNP simulations as much as possible. However, unlike in the case of the standard sources, the radioactivity dropped on the surface of the test source might diffuse into the ZrO₂ absorbent disk and thus be distributed along the depth. However, in our MCNP simulations we considered only the 2D distribution of radioactivity on the surface of the source that had been measured by radiochromic films. In addition, the stainless steel window film had to be welded to encapsulate the active source material. During electric welding, the quality and the shape of the window film was transformed by heat. These couldn't be described in the Monte Carlo simulations. These might contribute to the discrepancy between the radioactivities determined by this method and reported by the manufacturer.

<http://ie.lbl.gov/toi/>, Ver. 2.1, 2004.

REFERENCES

- [1] H. Haba, S. Motomura, Handbook of Nuclear Chemistry, Springer, New York City, USA, 2011.
- [2] M. Jackson, L. Nicola, Advances in Isotope Methods for the Analysis of Trace Elements in Man, CRC Press, London, England, 2001.
- [3] C. L. Chien, Radiochemistry in Nuclear Power Reactors, Radiochemical Techniques, National Academy Press, Washington D.C., USA, 1996.
- [4] J. M. Keller, Applied radiation measurements, Radioanalytical Chemistry, 134-162, 2007.
- [5] G. C. Lowenthal, Secondary standard instruments for the activity measurement of pure beta emitters, A Review, International Journal of Applied Radiation and Isotopes 20, 559-566, 1969.
- [6] J. M. R. Hutchinson, NIST measurement services, National Institute of Standards and Technology, Maryland, USA, 2004.
- [7] M. S. Patterson, R. C. Greene, Measurement of low energy beta-emitters in aqueous solution by liquid scintillation counting of emulsions, Analytical Chemistry 37 (7), 854-857, 1965.
- [8] B. R. S. Simpson, W. M. Van Wyngaardt, Activity measurements of the high-energy pure beta-emitters ⁸⁹Sr and ⁹⁰Y by the TDCR efficiency calculation technique, Applied Radiation and Isotopes 64, 1481- 1484, 2006.
- [9] C. H. Choi, S Jung, S-J. Ye, Radioactivity Determination of Sealed Beta-emitting Sources by Surface Dose Measurements and Monte Carlo Simulations, Transactions of the Korean Nuclear Society Spring Meeting, Korea, 2014.
- [10] C. H. Choi, H. S. Han, K-J Son, U. J. Park, J. S. Lee, W. R. Wee, S. W. Ha, I. H. Kim, S-J. Ye, Dosimetry of a new P-32 ophthalmic applicator, Medical Physics 38 (11), 6143 - 6151, 2011.
- [11] X-5 Monte Carlo Team, Los Alamos National Laboratory, MCNP—A general Monte Carlo N-particle transport code, Version 5, Los Alamos, USA, 2003.
- [12] D. R. Schaart, J. T. Jansen, J. Zoetelief, P. F. de Leege, A comparison of MCNP4C electron transport with ITS 3.0 and experiment at incident energies between 100 keV and 20 MeV: Influence of voxel size, substeps and energy indexing algorithm, Physics in Medicine and Biology 47, 1459-1484, 2002.
- [13] R. B. Firestone, L. P. Ekström, LBNL Isotope Project - LUNDS University WWW Table of Radioactive Isotopes,